Charge Carrier Mobility in Blends of Poly(9,9-dioctylfluorene) and Poly(3-hexylthiophene)

Amit Babel and Samson A. Jenekhe*

Department of Chemical Engineering and Department of Chemistry, University of Washington, Seattle, Washington 98195-1750

Received May 28, 2003; Revised Manuscript Received August 2, 2003

ABSTRACT: A series of 10 binary blends of poly(9,9-dioctylfluorene) and regioregular poly(3-hexylthiophene) were investigated and found to be phase separated and to exhibit high field-effect mobility of holes. The mobility of holes determined from blend thin film transistors was in the range of $2.0 \times 10^{-4}-1 \times 10^{-3}$ cm^2/(V s) in blends of 10−80 wt % poly(9,9-dioctylfluorene). A concave-upward dependence of hole mobility on blend composition was found with a minimum in mobility around the symmetric blend composition (50 wt %). The field-effect mobility of holes in poly(9,9-dioctylfluorene) homopolymer could not be determined directly because of the barrier to charge injection from gold electrodes. However, from the composition-dependent field-effect mobility of holes in the series of binary blends, we estimated the hole mobility in poly(9,9-dioctylfluorene) homopolymer to be $(6-10) \times 10^{-4}$ cm^2/(V s), which is in good agreement with previous results obtained by the time-of-flight technique. These results demonstrate that relatively high field-effect mobility of charge carriers can be realized in blends of conjugated polymers of current interest for various plastic electronic applications.

Introduction

The era of *plastic electronics* is emerging based on conjugated polymer semiconductors as active elements in electronic and photonic devices[1] including light-emitting diodes for displays,[1−4] thin-film transistors,[5,6] and photovoltaic cells.[7] Blends of conjugated polymers represent an attractive approach to optimizing and tuning the properties of the materials for device applications.[8,9] However, through blending of two or more conjugated polymers, a variety of novel phenomena and properties can emerge[8−10] as a result of intermolecular interactions, self-organization, or confinement effects, necessitating systematic compositional dependence studies. Here we will focus on charge carrier transport in binary blends of conjugated polymers.

Polyfluorene homopolymers, copolymers, and blends are currently of wide interest as electroluminescent materials for light-emitting diodes (LEDs).[3,11,12] Blue LEDs have been achieved using poly(9,9-dioctylfluorene) (PFO).[3] Other LED colors have been demonstrated based on PFO copolymers and other polyfluorene derivatives.[3,11] Although the solid-state fluorescence quantum yields of polyfluorenes are generally high (>50%),[3c] the electroluminescence (EL) efficiency is relatively low (∼0.2%) apparently because of charge injection limitations due to the high ionization potential (IP = 5.6−5.8 eV)[13a,b] and low electron affinity (EA = 2.1−2.6 eV)[13a,b] of PFO. Time-of-flight (TOF) measurements have showed that PFO and many of its copolymers have nondispersive hole transport with hole mobility in the $10^{-4}-10^{-3}$ cm^2/(V s) range at room temperature.[14] Dispersive electron transport with electron mobility of order 10^{-3} cm^2/(V s) has also been reported in a green electroluminescent PFO copolymer, poly(9,9-dioctylfluorene-*co*-benzothiadiazole).[15] According to these TOF studies, PFO and its copolymers have high carrier mobilities. However, none of these studies report charge transport-limited current, indicating nonohmic electrode contact with PFO. These charge injection limitations may explain why the field-effect mobility of carriers in polyfluorenes has not been reported except in chain aligned poly(9,9-dioctylfluorene-*co*-bithiophene) in a liquid crystalline phase.[5c] In contrast, rather high field-effect mobility of holes (0.02−0.1 cm^2/(V s)) in solution-cast regioregular poly(3-hexylthiophene) has been reported by several groups.[5,6c] Charge carrier transport studies based on thin-film field-effect transistors fabricated from blends or copolymers of polyfluorenes are important for understanding the roles and limitations of charge injection and transport in organic electronic devices.

In this paper, we report the morphology and the charge carrier mobility of a series of binary blends of poly(9,9-dioctylfluorene) (PFO) and regioregular poly(3-hexylthiophene) (PHT) whose structures are shown in Figure 1. The compositional dependence of charge carrier mobility in the PFO−PHT blend system was investigated by using the thin-film field-effect transistor (FET) as a platform. Atomic force microscopy (AFM) was used to investigate the blend morphology. The photophysical properties of the series of binary blends were characterized. The compositional dependence of the field-effect mobility of holes in the PFO−PHT blend system also provided a means to estimate the field-effect mobility of holes in the PFO homopolymer for the first time.

Experimental Section

Materials. The regioregular PHT sample with head-to-tail (HT) coupling exceeding 98.5% ($M_n \sim 12\,200$) and PFO ($M_w \sim 10\,000$) were purchased from Aldrich and American Dye Source, Inc., respectively. High-purity HPLC grade chloroform was used for making polymer solutions and the binary blends.

A series of 10 binary blends of PHT and PFO (10, 20, 30, 40, 50, 60, 70, 80, 90, and 95 wt % PFO) were prepared by mixing the appropriate volumes of 0.5 wt % solution in chloroform of each homopolymer. Composition of blends in this paper refers to weight percentage (or weight fraction, x) of PFO. All thin films of the homopolymers and blends were spin-

* To whom correspondence should be sent: e-mail jenekhe@cheme.washington.edu.

10.1021/ma034717t CCC: $25.00
Published on Web 09/13/2003

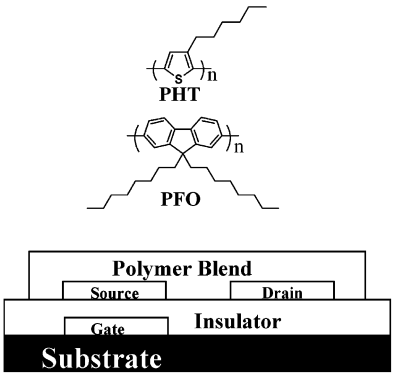

Figure 1. Molecular structures of binary blend components (PHT and PFO) and a schematic of the thin film transistor.

coated from chloroform solutions at a spin rate of 1000 rpm for 30 s. Residual solvent was removed by heating the samples in vacuo for 10−12 h at 60 °C. Blend thin films (20−30 nm thick) spin-coated on glass slides for optical measurements were homogeneous and showed good optical transparency.

Atomic Force Microscopy of Polymer Thin Films. The thin-film morphology of PHT and PFO homopolymers and their blends was studied using atomic force microscopy (AFM) (Digital Instruments, Santa Barbara, CA) in standard tapping mode. The thin films were spin-coated from their chloroform solutions onto Si substrate with a 300 nm SiO_2 in order to simulate the field-effect transistor structure. The film thickness of the polymer samples used for AFM imaging was 20−30 nm. The film thickness was measured by an Alpha-Step 500 profilometer (KLA-Tencor, Mountain View, CA) with an accuracy of 1 nm.

Optical Absorption and Photoluminescence Spectroscopy. Optical absorption spectra were obtained by using a Perkin-Elmer Lambda 900 UV/vis/near-IR spectrophotometer. Steady-state photoluminescence (PL) studies were carried out on a Spex Fluorolog-2 spectrofluorimeter. The films were positioned such that the emitted light was detected at 22.5° from the incident beam. Further details of the photophysical characterization are similar to our previous reports.[4f,g,9]

Fabrication and Characterization of Thin-Film Transistors. The thin-film field-effect transistors (FETs) were fabricated using a bottom contact geometry, as shown in Figure 1. Heavily doped Si with a conductivity of 10^3 S/cm was used as a gate electrode with a 300 nm thick SiO_2 layer as the gate dielectric. Using photolithography and vacuum sputtering system (2×10^{-6} Torr), two 90 nm thick gold electrodes (source and drain) with 10 nm thick TiW alloy adhesive layer were fabricated onto the SiO_2/Si substrates. A channel length (L) of 25 μm and a channel width (W) of 500 μm were used. A gold contact pad was also deposited on the gate electrode to make ohmic contact. Finally on top of this device structure thin films (20−30 nm) of the conjugated polymers or their binary blends were spin-coated from chloroform solutions and dried overnight (10−12 h) at 60 °C in a vacuum oven. Electrical characteristics of the devices were measured using an HP 4155A semiconductor parameter analyzer (Yokogawa Hewlett-Packard, Tokyo). All the measurements were done under ambient laboratory conditions.

Results and Discussion

Morphology of PFO−PHT Blends. The morphology of PFO−PHT blend thin films on SiO_2/Si substrates was investigated using atomic force microscopy (AFM) in standard tapping mode. Figure 2 shows the 5 μm × 5 μm topographic images of the blends as a function of composition. Figure 2a is a micrograph of the 10 wt % PFO blend. Spherical cluster-like features having an average size of 250 nm and a height of 10−15 nm are distributed throughout the image, indicating a phase-separated blend system. On increasing the concentration of PFO from 10 to 50 wt %, there is a slight increase in the cluster size (Figure 2a−c). Beyond 50 wt % PFO, the clusters increase in size but decrease in number, as can be seen from the images of the 50, 70, and 90 wt % PFO blends (Figure 2c−e). These AFM images which show spherical domains distributed in a matrix suggest that the demixing in the binary PFO−PHT blends is by nucleation and growth.

Photophysical Properties of PFO−PHT Blends. The optical absorption and the photoluminescence (PL) emission spectra of thin films of PHT and PFO homopolymers are shown in Figure 3. PHT has absorption maxima at 560 nm and an absorption band edge around 650 nm (1.9 eV). PFO has absorption maxima at 380 nm with a shoulder at 435 nm and an absorption band edge around 445 nm (2.8 eV). The emission spectrum of PFO (380 nm excitation) has a well-resolved vibronic structure with peaks at 436, 462, and 493 nm. In contrast, the emission spectrum of PHT (560 nm excitation) has a peak at 650 nm and a minor peak at 715 nm. The PL emission band of PFO is seen to completely overlap the absorption band of PHT. This suggests that Förster energy transfer from PFO to PHT can be expected.

The absorption spectra of the PFO−PHT binary blends are shown in Figure 4a. They are simple superpositions of those of their parent homopolymers. New absorption features were not observed in the wavelength range from 300 to 800 nm, suggesting that there is no evidence of strong ground-state interaction or charge transfer between the two blend components. The shoulder peak at 435 nm in the absorption spectrum of PFO homopolymer (Figure 3), which is due to chain aggregation,[16] is also reproduced in the blend absorption spectra. This observation is in good agreement with the phase-separated morphology revealed by AFM images.

The PL emission spectra of the PFO−PHT blends, normalized with respect to the PHT emission peak at 650 nm, are shown in Figure 4b. The same blend PL emission spectra, when normalized relative to the PFO emission peak at 436 nm, are shown in Figure 4c. It can be seen that the emission spectra of the blends are composed of contributions from both PFO and PHT. Increasing the concentration of one of the blend components results in a relative increase in PL peak intensity of that component and corresponding decrease in PL intensity of the other component. The relative PL quantum efficiency of the 50 wt % blend, for example, was decreased by 80% compared to that of the 95 wt % PFO blend. The observed enhancement in the intensity of the PHT emission band (Figure 4c) in the blends suggest some energy transfer from PFO to PHT. We note that the additional green emission band commonly found in the PL and EL spectra of PFO[3e,11,16] is completely absent in the blend PL spectra (Figure 4).

PFO−PHT Blend Thin-Film Transistors. The output characteristics (plot of drain current I_d vs drain voltage V_d at different gate voltages V_g) of the devices showed typical p-channel field-effect transistor accumulation mode behavior.[17] The field-effect mobility of holes was calculated from the slope of $I_d^{1/2}$ vs V_g (transfer characteristic). Field-effect transistors (FETs) fabricated from the PHT homopolymer under the same conditions as used for the blend FETs gave the field-effect mobility of holes in the 0.008−0.02 $cm^2/(V\ s)$ range with I_{on}/I_{off} ratio of 10^4. These results are in close agreement with the reported hole mobility of regioregu-

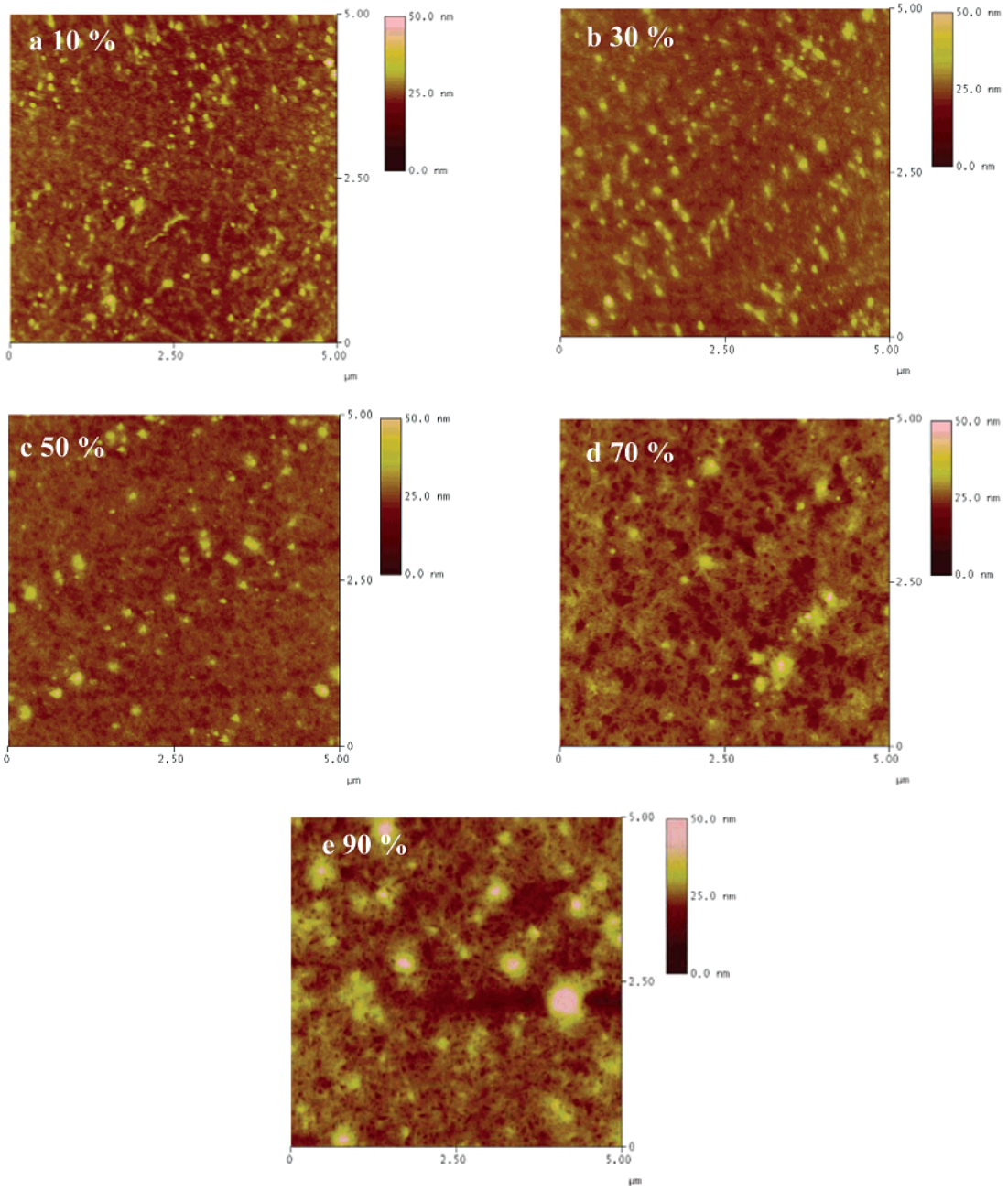

Figure 2. AFM tapping mode topographic images of 10% (a), 30% (b), 50% (c), 70% (d), and 90% (e) PFO blend thin films on SiO_2 surface on a silicon substrate.

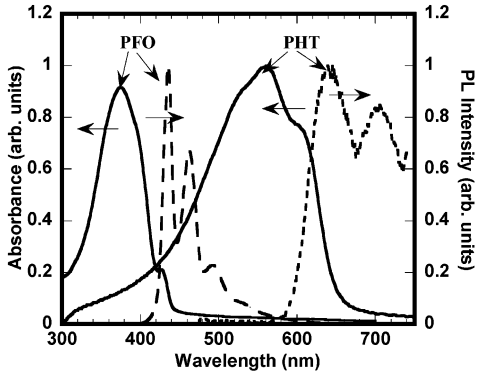

Figure 3. Normalized thin film optical absorption and PL emission spectra of PHT and PFO homopolymers.

lar PHT for devices fabricated under similar conditions.[5a,6c] The field-effect mobility of carriers could not be measured in PFO homopolymer FET devices. However, the field-effect mobility of holes in PFO homopolymer was estimated to be in the range of $(6-10) \times 10^{-4}$ cm^2/(V s) by extrapolation of the blend composition-dependent hole mobility data discussed below. This estimated hole mobility in PFO homopolymer is in good agreement with the time-of-flight hole mobility (4×10^{-4} cm^2/(V s)) reported for unaligned PFO films.[14]

All of the 10 blend compositions from $x = 0.1$ to 0.95 (x is the weight fraction of PFO) showed typical p-channel FET characteristics. The devices were air-stable, allowing determination of the hole mobility under ambient air conditions. Representative FET output and transfer characteristics are shown in Figures 5−7 for blends with $x = 0.1$, 0.4, and 0.6. The field-effect hole mobility of the 10 wt % blend calculated from the saturation region of Figure 5 was 1×10^{-3} cm^2/(V s), and the corresponding I_{on}/I_{off} ratio was 400. Similar

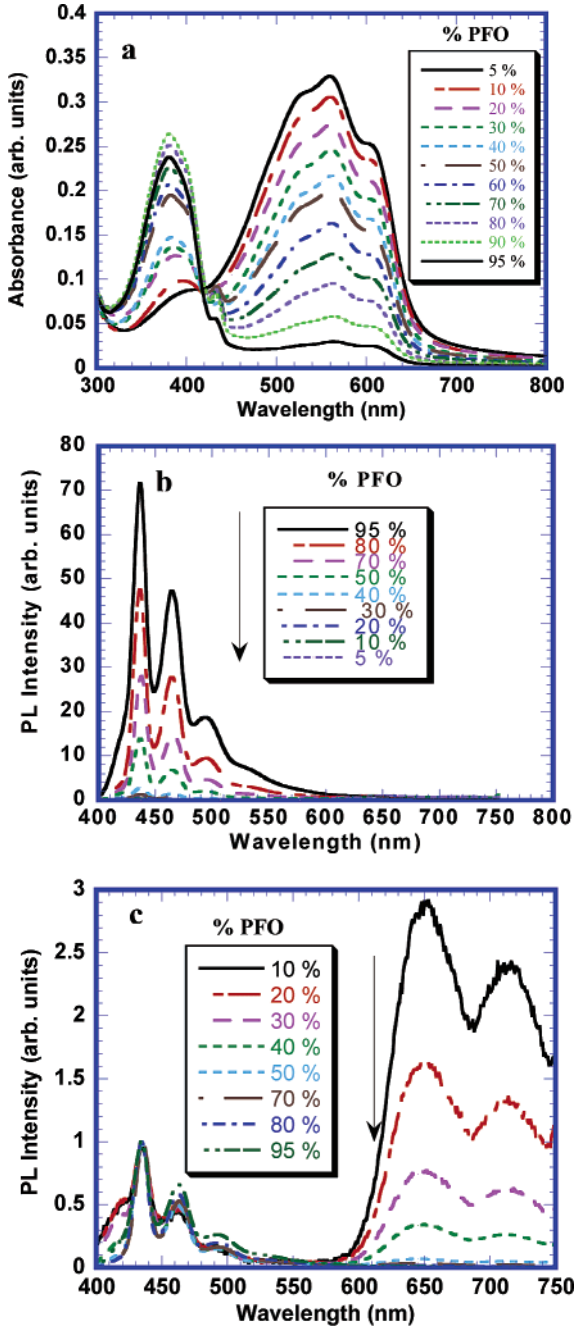

Figure 4. UV−vis absorption (a) and PL emission spectra (b, c) of PFO−PHT blends. Normalized PL emission with respect to PHT emission peak at 650 nm (b) and with respect to PFO emission peak at 436 nm (c).

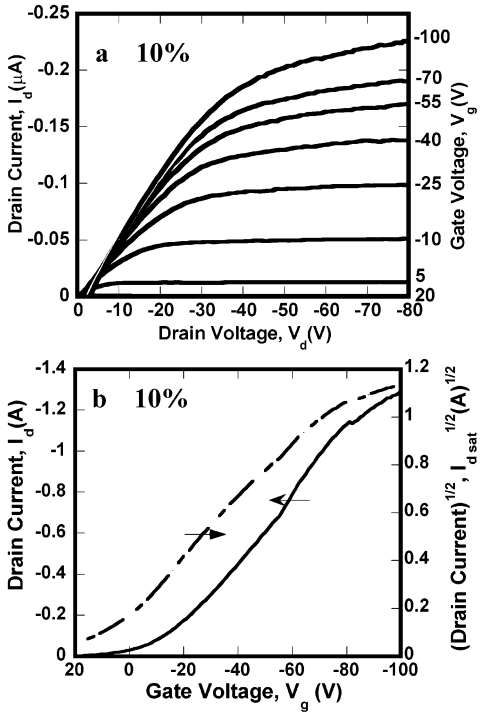

Figure 5. Output (a) and transfer characteristics (b) of a 10 wt % PFO blend FET with $W = 500$ μm and $L = 25$ μm.

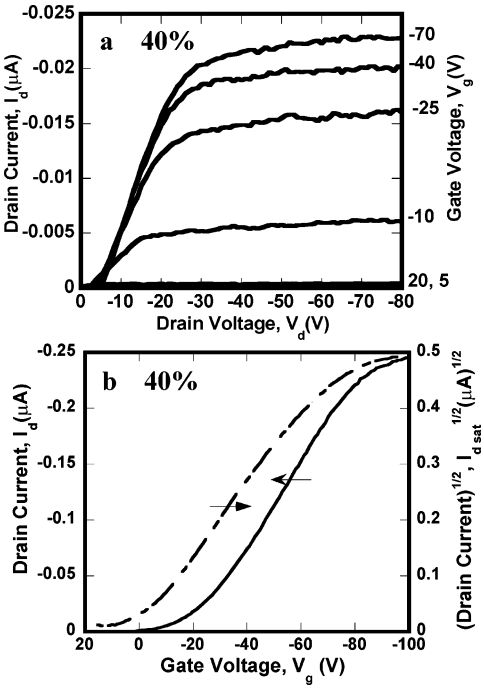

Figure 6. Output (a) and transfer characteristics (b) of a 40 wt % PFO blend FET with $W = 500$ μm and $L = 25$ μm.

results for the 40 wt % PFO blend (Figure 6) were 2.4 $\times$ 10^{-4} cm^2/(V s) and 1100, respectively, whereas for the 60 wt % PFO blend (Figure 7), the values were 2.2 $\times$ 10^{-4} cm^2/(V s) and 700.

The compositional dependence of the field-effect mobility of holes in the PFO−PHT blend system is shown in Figure 8. A shallow concave-upward dependence was observed in the blends, with a minimum in the field-effect mobility at around the symmetric blend composition (50 wt %). On adding just 10 wt % of PFO in PHT, which is the higher mobility component, the hole mobility in the blend is reduced by more than 1 order of magnitude to 1 $\times$ 10^{-3} cm^2/(V s). This rather huge decrease in hole mobility by just adding "impurity" amount (10 wt %) of PFO in PHT is likely due to the effects of hole blocking by PFO. Since the difference in ionization potential of PFO (IP = 5.6−5.8 eV)[13a,b] and PHT (IP = 5.2 eV)[13c] is 0.4−0.6 eV, this represents a barrier to hole injection into PFO from PHT. Since holes cannot be trapped by PFO within the matrix of PHT the reduction in hole mobility arises from the decrease in hopping rate due to the presence of the PFO barriers. Further increase of PFO concentration in the blend results in increase in size and number of these hole blocking clusters within PHT. Consequently, a decrease in the hole mobility to 2 $\times$ 10^{-4} cm^2/(V s) in the 50 wt

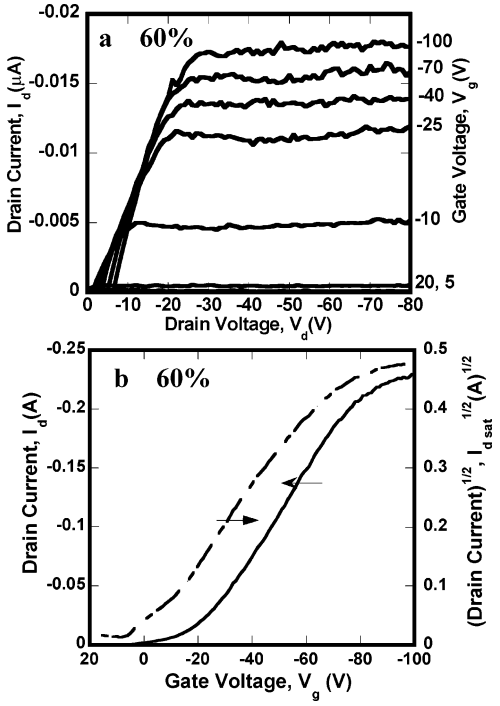

Figure 7. Output (a) and transfer characteristics (b) of a 60 wt % PFO blend FET with $W = 500$ μm and $L = 25$ μm.

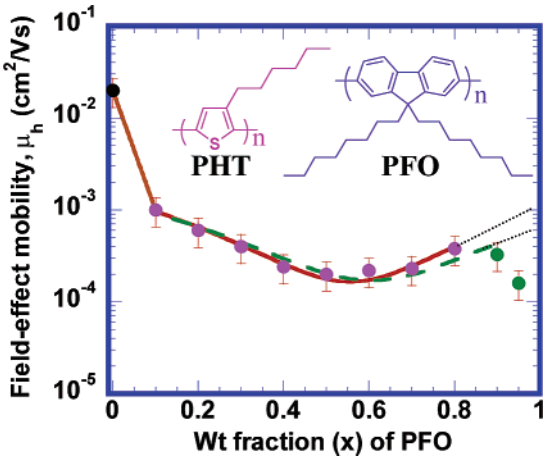

Figure 8. Compositional dependence of the field-effect mobility of holes in PFO−PHT blends. The solid line is a quadratic fit for $0.1 \leq x \leq 0.8$, and the dashed line is a quadratic fit for $0.1 \leq x \leq 0.9$.

% PFO blend is observed. Above 50 wt % PFO, however, the hole mobility in going from 50 wt % (2×10^{-4} cm^2/(V s)) to 80 wt % PFO (4×10^{-4} cm^2/(V s)) is seen to increase slightly. Since PFO is a liquid crystalline polymer that tends to be highly ordered in thin films,[11] the PFO-rich blends are likely to be more ordered than the 50 wt % blend. Such PFO-rich blends can thus provide a template for ordering the minority PHT phase, facilitating the observed enhanced carrier mobility in the 80 wt % PFO blend.

The hole mobility in blends with PFO content greater than 90 wt % decreased slightly to about 2×10^{-4} cm^2/(V s). The field-effect mobility of holes could not be measured in PFO−PHT blends with PFO concentration exceeding 95 wt % or in PFO homopolymer thin film. This decrease in the mobility and inability to measure the hole mobility in PFO homopolymer are likely a result of charge injection difficulties. It has been shown that, for PFO thin films, Au electrode shows typical blocking behavior or injection-limited contact.[18a] We note that the barrier for injecting holes into PFO from either Au or PHT is the same (0.4−0.6 eV), since the ionization potential of PHT and the work function of Au are identical (5.2 eV). Although this injection barrier can be considered small enough for the contact to be ohmic, it is well-known that the metal/polymer interface plays a crucial role in making a contact ohmic or blocking.[18] Therefore, given that in the present case the Au/PFO−PHT blend contact is largely blocking in the 90−95 wt % PFO blends, a nonlinear regression of the $\mu(x)$ data was done with and without the 90 wt % data point.[19] By extrapolating the best fit of the mobility−composition, $\mu(x)$, data for the blends to $x = 1$, we obtained estimates of the field-effect mobility of holes in PFO homopolymer to be $(6-10) \times 10^{-4}$ cm^2/(V s), which is in good agreement with the hole mobility obtained by the time-of-flight method.[14]

The compositional dependence of the charge carrier mobility $\mu(x)$ in Figure 8 clearly does not follow an exponential function of the form $\mu(x) = \mu_0 \exp(-ax)$ or a similar power law expected if the charge transport is described by the energetic disorder controlled hopping model.[20] Hole transport in the PFO−PHT blend system is not described by percolation type models[20] since both components have a nonzero charge carrier mobility. The observed concave-upward appearance of compositional dependence of hole mobility in PFO−PHT blends is also very different from a characteristic three-regime "stair-step" dependence of the field-effect mobility on blend composition found for electrons in poly(benzobisimidazobenzophenanthroline)/poly(*p*-phenylene-2,6-benzobisthiazole) blend system[6b] and for holes in binary blends of poly(3-hexylthiophene) and poly(3-decylthiophene).[6c] The above polynomial fit[19] of the $\mu(x)$ data has no theoretical basis but was simply an approach to estimate the otherwise inaccessible field-effect mobility of holes in the PFO homopolymer. One of the important issues highlighted by the present and other recently reported $\mu(x)$ data[6b] is that charge carrier transport in blends of conjugated polymer semiconductors is not explained by current theoretical models.[20]

The observed relatively high charge carrier mobility (ca. $(2-10) \times 10^{-4}$ cm^2/(V s)) in all of the blend compositions ($0.1 \leq x \leq 0.95$) makes conjugated polymer blend FETs useful and attractive by offering the prospect of integration of different properties of polymers such as light emission, photoresponse, or sensing with good transistor characteristics. Furthermore, the novel form of the compositional dependence of the hole mobility in these blends (Figure 8) suggests that studies of blends of conjugated polymers will enlarge our knowledge of charge transport in organic semiconductors.

Conclusions

Binary blends of PFO and regioregular PHT were found to be phase separated and to exhibit relatively high field-effect mobility of holes in thin film field-effect transistors. A concave-upward compositional dependence of hole mobility was found with an initial decrease in mobility from 0.02 cm^2/(V s) in PHT homopolymer to 2×10^{-4} cm^2/(V s) in the 50 wt % blend, when PFO is present as a minor component, and followed by an increase to 4×10^{-4} cm^2/(V s) in the 80 wt % blend. By extrapolating the best fit of the mobility−composition data to $x = 1$, the field-effect mobility of holes in PFO homopolymer was estimated to be in the $(6-10) \times 10^{-4}$

$cm^2/(V\ s)$ range. This value of the hole mobility in PFO is in very good agreement with that measured by the time-of-flight method. The lack of field-effect transistor characteristics in PFO homopolymer whereas high mobility of holes is observed in PFO−PHT blends demonstrates the critical role of charge injection in thin film transistors and other organic electronic devices.

Acknowledgment. This research was supported by the Air Force Office of Scientific Research (Grant F49620-03-1-0162) and in part by the U.S. Army Research Laboratory and the U.S. Army Research Office (Grant DAAD-19-01-1-0676) and the Boeing-Martin Professorship Endowment.

References and Notes

(1) (a) Heeger, A. J. *Angew. Chem., Int. Ed.* **2001**, *40*, 2591. (b) MacDiarmid, A. G. *Angew. Chem., Int. Ed.* **2001**, *40*, 2581.

(2) (a) Kraft, A.; Grimsdale, A. C.; Holmes, A. B. *Angew. Chem., Int. Ed.* **1998**, *37*, 402. (b) Bernius, M. T.; Inbasekaran, M.; O'Brien, J.; Wu, W. *Adv. Mater.* **2000**, *12*, 1737.

(3) (a) Ohmori, Y.; Uchinda, M.; Muro, K.; Yoshino, K. *Jpn. J. Appl. Phys.* **1991**, *30*, L1941. (b) Pei, Q.; Yang, Y. *J. Am. Chem. Soc.* **1996**, *118*, 7416. (c) Grice, A. W.; Bradley, D. D. C.; Bernius, M. T.; Inbasekaran, M.; Wu, W. W.; Woo, E. P. *Appl. Phys. Lett.* **1998**, *73*, 629. (d) Herguth, P.; Jiang, X.; Liu, M. S.; Jen, A. K.-Y. *Macromolecules* **2002**, *35*, 6094. (e) Kulkarni, A. P.; Jenekhe, S. A. *Macromolecules* **2003**, *36*, 5285.

(4) (a) Sokolik, I.; Yang, Z.; Karasz, F. E.; Morton, D. C. *J. Appl. Phys.* **1993**, *74*, 3584. (b) Peng, Z.; Bao, Z.; Galvin, M. E. *Chem. Mater.* **1998**, *10*, 2086. (c) Jenekhe, S. A.; Zhang, X.; Chen, X. L.; Choong, V.-E.; Gao, Y.; Hsieh, B. R. *Chem. Mater.* **1997**, *9*, 409. (d) Tarkka, R. M.; Zhang, X.; Jenekhe, S. A. *J. Am. Chem. Soc.* **1996**, *118*, 9438. (e) Zhang, X.; Shetty, A. S.; Jenekhe, S. A. *Acta Polym.* **1998**, *49*, 52. (f) Zhang, X.; Shetty, A. S.; Jenekhe, S. A. *Macromolecules* **1999**, *32*, 7422. (g) Zhang, X.; Jenekhe, S. A. *Macromolecules* **2000**, *33*, 2069. (h) Alam, M. M.; Jenekhe, S. A. *Chem. Mater.* **2002**, *14*, 4775.

(5) (a) Bao, Z.; Dodabalapur, A.; Lovinger, A. J. *Appl. Phys. Lett.* **1996**, *69*, 4108. (b) Sirringhaus, H.; Tessler, N.; Friend, R. H. *Science* **1998**, *280*, 1741. (c) Sirringhaus, H.; Wilson, R. J.; Friend, R. H.; Inbasekaran, M.; Wu, W.; Woo. E. P.; Grell, M.; Bradley, D. D. C. *Appl. Phys. Lett.* **2000**, *77*, 406.

(6) (a) Babel, A.; Jenekhe, S. A. *Adv. Mater.* **2002**, *14*, 371. (b) Babel, A.; Jenekhe, S. A. *J. Phys. Chem. B* **2002**, *106*, 6129. (c) Babel, A.; Jenekhe, S. A. *J. Phys. Chem. B* **2003**, *107*, 1749.

(7) (a) Yu, G.; Heeger, A. J. *J. Appl. Phys.* **1995**, *78*, 4510. (b) Arias, A. C.; MacKenzie, J. D.; Stevenson, R.; Halls, J. J. M.; Inbasekaran, M.; Woo, E. P.; Richards, D.; Friend, R. H. *Macromolecules* **2001**, *34*, 6005. (c) Antoniadis, H.; Hsieh, B. R.; Abkowitz, M. A.; Jenekhe, S. A.; Stolka, M. *Synth. Met.* **1994**, *62*, 265. (d) Jenekhe, S. A.; Yi, S. *Appl. Phys. Lett.* **2000**, *77*, 2635.

(8) (a) Yu, G.; Nishino, H.; Heeger, A. J.; Chen, T.-A.; Rieke, R. D. *Synth. Met.* **1995**, *72*, 249. (b) Chen, X. L.; Jenekhe, S. A. *Macromolecules* **1997**, *30*, 1728. (c) Jenekhe, S. A.; de Paor, L. R.; Chen, X. L.; Tarkka, R. M. *Chem. Mater.* **1996**, *8*, 2401.

(9) (a) Zhang, X.; Kale, D. M.; Jenekhe, S. A. *Macromolecules* **2002**, *35*, 382. (b) Alam, M. M.; Tonzola, C. J.; Jenekhe, S. A. *Macromolecules* **2003**, *36*, 6577.

(10) (a) Berggren, M.; Inganas, O.; Gustafsson, G.; Rasmusson, J.; Andersson, M. R.; Hjertberg, T.; Wennerstrom, O. *Nature (London)* **1994**, *372*, 444. (b) Jenekhe, S. A.; Osaheni, J. A. *Science* **1994**, *265*, 765. (c) Osaheni, J. A.; Jenekhe, S. A. *Macromolecules* **1994**, *27*, 739. (d) Jenekhe, S. A.; Yi, S. *Adv. Mater.* **2000**, *12*, 1274.

(11) (a) Neher, D. *Macromol. Rapid Commun.* **2001**, *22*, 1365−1385. (b) Scherf, U.; List, E. J. W. *Adv. Mater.* **2002**, *14*, 477.

(12) (a) He, G.; Liu, J.; Li, Y.; Yang, Y. *Appl. Phys. Lett.* **2002**, *80*, 1891. (b) Palilis, L. C.; Lidzey, D. G.; Redecker, M.; Bradley, D. D. C.; Inbasekaran, M.; Woo, E. P.; Wu, W. W. *Synth. Met.* **2001**, *121*, 1729. (c) Sainova, D.; Miteva, T.; Nothofer, H. G.; Scherf, U.; Glowacki, I.; Ulanski, J.; Fujikawa, H.; Neher, D. *Appl. Phys. Lett.* **2000**, *76*, 1810.

(13) (a) Liao, L. S.; Fung, M. K.; Lee, C. S.; Lee, S. T.; Inbasekaran, M.; Woo, E. P.; Wu, W. W. *Appl. Phys. Lett.* **2000**, *76*, 3582. (b) Janietz, S.; Bradley, D. D. C.; Grell, M.; Giebler, C.; Inbasekaran, M.; Woo, E. P. *Appl. Phys. Lett.* **1998**, *73*, 2453. (c) Onoda, M.; Tada, K.; Zakhidov, A. A.; Yoshino, K. *Thin Solid Films* **1998**, *331*, 76.

(14) Redecker, M.; Bradley, D. D. C.; Inbasekaran, M.; Woo, E. P. *Appl. Phys. Lett.* **1998**, *73*, 1565.

(15) Campbell, A. J.; Bradley, D. D. C.; Antoniadis, H. *Appl. Phys. Lett.* **2001**, *79*, 2133.

(16) (a) Bradley, D. D. C.; Grell, M.; Long, X.; Mellor, H.; Grice, A. *Proc. SPIE* **1997**, *3145*, 254. (b) Gaal, M.; List, E. J. W.; Scherf, U. *Macromolecules* **2003**, *36*, 4236.

(17) (a) Sze, S. M. *Physics of Semiconducting Devices*; Wiley: New York, 1981. (b) Horowitz, G. *Adv. Mater.* **1998**, *10*, 365. (c) In the saturation regime ($V_d > V_g - V_t$, where V_t is the threshold voltage), I_d can be described using the equation $I_d = (W/2L)C_0\mu(V_g - V_t)^2$, where μ is the field-effect mobility, W is the channel width, L is the channel length, and C_0 is the capacitance per unit area of the gate dielectric layer (SiO_2, 300 nm, $C_0 = 11$ nF/cm^2).

(18) (a) Campbell, A. J.; Bradley, D. D. C.; Antoniadis, H. *J. Appl. Phys.* **2001**, *89*, 3343. (b) Ioannidis, A.; Facci, J. S.; Abkowitz, M. A. *J. Appl. Phys.* **1998**, *84*, 1439.

(19) The hole mobility for most of the blend composition (10−80 wt % PFO) was found to be well described by a quadratic expression: $\mu_h = 0.0013 - 0.0043x + 0.004x^2$, with $R = 0.99$. Another fit was done with the following expression for 10−90 wt % PFO blends: $\mu_h = 0.0012 - 0.0036x + 0.003x^2$, which gives an R value of 0.96.

(20) (a) Van der Auweraer, M.; De Schryver, F. C.; Borsenberger, P. M.; Bassler, H. *Adv. Mater.* **1994**, *6*, 199. (b) Borsenberger, P. M.; Weis, D. S. *Organic Photoreceptors for Imaging Systems;* Marcel Dekker: New York, 1993.

MA034717T